

# Design and Optimization of A Direct-Conversion Double-Balanced Mixer for RF Receiver Front-End

Frederick Ray I. Gomez

New Product Introduction Department, Back-End Manufacturing & Technology, STMicroelectronics, Inc.  
9 Mountain Drive, Light Industry & Science Park II, Brgy. La Mesa, Calamba City, Laguna, Philippines 4027

**Abstract:** Differential implementation is becoming highly favoured in RFIC (radio frequency integrated circuit) design, notably its high immunity to common-mode noises, acceptable rejection of parasitic coupling, and increased dynamic range. One specific RF front-end building block that is usually designed as a differential circuit is the mixer. This technical paper presents a study of a differential mixer, notably the double-balanced mixer implemented on a direct-conversion architecture in a standard 90nm CMOS (complementary metal-oxide semiconductor) process. Operating frequency is set at 5GHz, which is a typical frequency for RF (radio frequency) receiver. Impedance matching was essential to fully optimize the mixer design. The direct-conversion double-balance mixer design eventually achieved conversion gain of 11.463dB and noise figure of 16.529dB, comparable to mixer designs from past research and studies.

**Keywords:** Double-Balanced Mixer; Direct Conversion; Conversion Gain; Noise Figure; RF Front-End

## 1. Introduction

The front-end of a RF (radio frequency) wireless receiver is of particular interest to many RFIC (radio frequency integrated circuit) designers and researchers as it attests to be the most critical part in many communication systems and wireless applications like the Bluetooth, WiFi (wireless fidelity), and WiMAX (worldwide interoperability for microwave access). The block diagram of a typical receiver is shown in **Figure 1**.

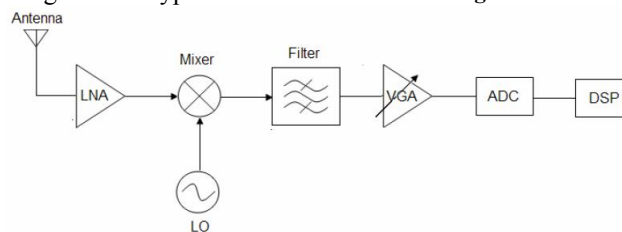


**Figure 1;** Block diagram of a typical RF receiver.

Mixer is among the front-end building blocks of an RF receiver. It is also referred to as a converter because it converts RF signals into a lower intermediate frequency (IF) by mixing with an offset local oscillator (LO). Depending on the RF receiver requirements, mixers must undergo a careful design process since complex tradeoffs exists among different performance parameters.

## 2. Review of Related Literature

RF receivers can be categorized as superheterodyne (high-IF), low-IF, and homodyne or direct-conversion or zero-IF based on the resulting IF signal they operate. For the direct-conversion receiver, IF is designed to be centered

Copyright © 2018 Frederick Ray I. Gomez  
doi: 10.18063/pee.v1i3.800

This is an open-access article distributed under the terms of the Creative Commons Attribution Unported License (<http://creativecommons.org/licenses/by-nc/4.0/>), which permits unrestricted use, distribution, and reproduction in any medium, provided the original work is properly cited.

at frequency zero. This means that the LO frequency is equal to the input RF frequency. With zero-IF, image signal is avoided and the analog filtering problem can be easily handled. Moreover, the desired signal is translated directly to the baseband, allowing analog-to-digital converter (ADC) and digital signal processing (DSP) circuits to perform modulation and other supplementary functions<sup>[1,2]</sup>. This eliminates the need for highly complex filters since channel selection only requires a low-pass filter (LPF) as shown in **Figure 2**. Smaller and cheaper receivers with low power consumption could be realized for various wireless applications such as Bluetooth, WiFi, and WiMAX. Many of the implemented receivers in WiMAX<sup>[3-5]</sup> use the zero-IF architecture since the LPFs make sure that the closely-spaced carrier signals do not cause interference with each other.

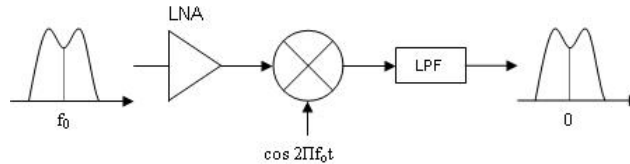


**Figure 2;** Direct-conversion or zero-IF receiver.

Designing a mixer must take into account the trade-offs among the performance parameters. As earlier mentioned, a careful study of these important parameters must be done in order to design a fully-functional and optimized mixer. A mixer's efficiency on frequency conversion from RF to IF is characterized by conversion gain (CG) or loss, expressed in Eq. (1) and (2). CG is the ratio of the desired IF output to the value of the RF input, and may be expressed in voltage or power. In cases when CG is less than unity or 0dB, it is fittingly termed as a conversion loss.

$$CG_{voltage} = 20 \log \frac{V_{IF}}{V_{RF}} \quad \text{Eq. (1)}$$

$$CG_{power} = 10 \log \frac{P_{IF}}{P_{RF}} \quad \text{Eq. (2)}$$

$V_{IF}$  and  $V_{RF}$  are the root mean square (RMS) voltages of the IF and RF signals, respectively, while  $P_{IF}$  and  $P_{RF}$  are the equivalent power of the IF and RF signals, respectively. Conversion gain is preferred over conversion loss because amplification along with frequency translation. Nevertheless, it should be noted that conversion gain directly affects the noise figure and linearity of the overall receiver. Hence, design tradeoffs concerning these parameters are inevitable.

Noise figure (NF) is another important parameter of the mixer. It is a measure of the amount of signal-to-noise-ratio (SNR) degradation introduced by the mixer as seen at the output. Eq. (3) shows the relation between the SNR at the input port and the SNR at the output port of the mixer.

$$NF = 10 \log \left( \frac{SNR_{IN}}{SNR_{OUT}} \right) \quad \text{Eq. (3)}$$

Noise figures of mixers tend to be higher than amplifiers (i.e. low-noise amplifiers, power amplifiers) because of the contribution of noise from other frequencies (apart from input RF signal) that can mix down to the IF. This considerable noise in mixers is the main reason why low-noise amplifiers (LNA) are used in the front-end, before the mixer<sup>[6]</sup>.

A popular solution for the mixer is based on the double-balanced topology, with the schematic shown in **Figure 3**. Double-balanced mixer is also commonly known as Gilbert cell mixer. It operates with differential LO and RF inputs. In this topology, LO products are prevented from getting to the output by combining two single-balanced mixers. As illustrated in Figure 3, the two single-balanced mixers are connected in anti-parallel as far as the LO is concerned, but in parallel for the RF signal. Thus, the LO terms sum to zero in the output, whereas the converted RF signal is doubled in the output<sup>[6]</sup>. This is most desirable for high port-to-port isolation and spurious output rejection applications.

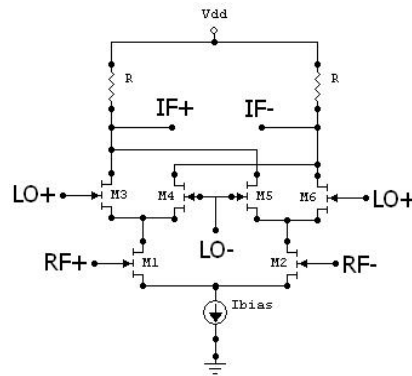


Figure 3; Double-balanced mixer topology.

### 3. Double-Balanced Mixer Design

Double-balanced mixer topology can provide high conversion gain, very low noise figure, and high degree of LO-IF isolation. The main disadvantage of this topology is its physical implementation. A balun transformer is required to convert the single-ended input to a differential RF input signal of the mixer. Transformers with very low insertion loss are difficult to realize in monolithic integration, hence this forces the use of an off-chip transformer which occupies more board space and cost<sup>[7]</sup>. An alternative solution is to use active baluns in place of their passive counterparts, as they can produce gain, occupy smaller chip area and can operate at RF and higher frequencies<sup>[8]</sup>.

The goal of the paper is then to design and optimize a direct-conversion double-balanced mixer implemented in a standard 90nm CMOS (complementary metal-oxide semiconductor) process, operating at frequency of 5GHz which is a typical frequency for an RF receiver. The target specifications of the figures of merit are based on the performance comparison in terms of conversion gain and noise figure of past researches on direct-conversion active mixer topologies given in **Table 1**.

Design	RF (GHz)	Conversion Gain (dB)	Noise Figure (dB)	Topology
[4]	3.4~3.85	10	10	Single-balanced
[5]	2~11	21.5~22.8	21.5~25.8	Double-balanced
[9]	2	19.5	10.2	BiCMOS Double-balanced
[10]	20~40	16	--	BiCMOS Single-balanced
[11]	5.2	9.3	10.5	Double-balanced

Table 1. Performance comparison of mixer designs.

It is imperative to determine the proper biasing and sizing of all the transistors such that RF transistors (M1-M2) will operate in the saturation region while the LO transistors (M3-M6) operate near the boundary of the saturation and linear regions. The mixer design used nsvt (NMOS standard Vt) which is the typical model for the transistor.

One way to increase the performance of the mixer in terms of conversion gain and noise figure is to apply impedance matching in the circuit.  $Z_{11}$  and  $Z_{22}$  can be obtained using sp-analysis which is swept from  $f_1 = 700\text{MHz}$  to  $f_2 = 6\text{GHz}$ . Actual inductor and capacitor values at  $f = 5\text{GHz}$  can be computed from the L-network reactances. Inductors and capacitors are key passive components that are crucial for impedance matching, and are specifically designed such that they would satisfy the conversion gain of the mixer. Impedance matching is necessary in RF circuit design to provide maximum possible power transfer between the source or the generator and the load<sup>[12]</sup>. The schematic diagram of the whole circuit is shown in **Figure 4**.

To supply differential LO input to the mixer, a port PORT2 with a matching resistor (set to  $50\Omega$ ) is used which is then fed into an ideal passive balun to convert the single-ended signal into differential. For the differential RF input of the mixer, same setup as the LO is used with PORT1. To use the differential output for measurements, matching the IF output port PORT3 to the output impedance of the mixer is necessary. PORT1 is set to DC source type with pacmag

(periodic ac magnitude) set to 1. PORT3, which is the IF port, is set also to DC source type. The only large signal is from PORT2 which is a sine wave with  $f_{LO}=5\text{GHz}$  and  $P_{LO}=0\text{dBm}$ .

For the impedance matching, the input matching network is applied before the differential RF input of the mixer instead of placing it before the balun. This will result to an adjustment on the value of  $L_1$ , which will decrease, since the balun circuit has self-inductance. The adjusted value of  $L_1$  can be determined using the sp-analysis swept from  $f_1 = 700\text{MHz}$  to  $f_2 = 6\text{GHz}$ . Moreover, inductors with small inductances are more realizable in actual designs than their larger counterparts. The final values of the L-matching network are summarized in **Table 2**.

Software design tools *ASITIC*<sup>[13,14]</sup> and *SpiralCalc*<sup>[15,16]</sup> were used for the design of the inductors. Both software tools are available for academic and non-commercial purposes. **Table 3** shows the design parameters obtained for the design of the spiral inductors using *ASITIC* while **Table 4** shows that of using *SpiralCalc*.

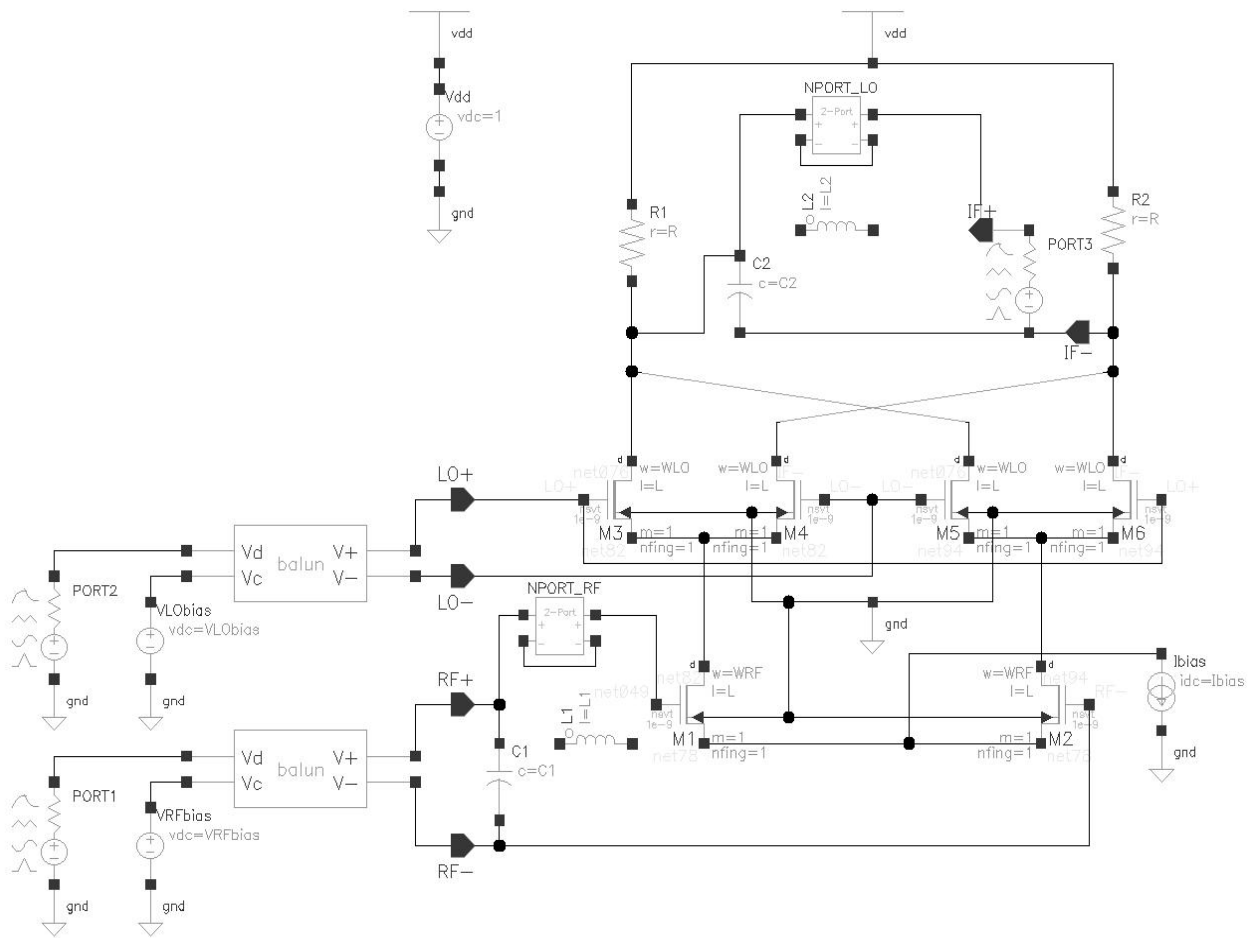


**Figure 4;** Schematic design of double-balanced mixer.

L and C	Value
$L_1$	12.7nH
$C_1$	1.116087pF
$L_2$	1.328515nH
$C_2$	267.127fF

**Table 2.** Final values of L-network elements.

Parameters	Inductors	
	L <sub>1</sub>	L <sub>2</sub>
Desired L	12.7nH	1.328515nH
No. of sides	4	8
Length, D	300μm	190μm
Metal width, W	10.886μm	10.901775μm
Spacing, S	1	1
No. of turns, N	4.25	2.5
Metal layer	7	7
Inductance, L	12.711nH	1.329nH
Q-factor, Q	2.322	5.694

**Table 3.** Inductor design using *ASITIC*.

Parameters	Inductors	
	L <sub>1</sub>	L <sub>2</sub>
Desired L	12.7nH	1.328515nH
No. of sides	4	8
Length, D	300μm	190μm
Metal width, W	11.2μm	10μm
Spacing, S	1	1
No. of turns, N	6	2
Inductance, L:		
Modified Wheeler	12.885μm	1.326μm
Current Sheet	12.739μm	1.326μm
Monomial Fit	12.624μm	1.394μm

**Table 4.** Inductor design using *SpiralCalc*.

In *ASITIC*, the spiral inductors are designed such that desired inductances are achieved and the Q-factors are optimized with eddy-current option enabled to include the effects of substrate induced eddy current losses. L<sub>1</sub> have smaller Q-factor than L<sub>2</sub> because of its high inductance value. For the inductor design using *SpiralCalc*, same parameter values from the *ASITIC* parameters are used except for the metal width and the number of turns of the spiral inductor. These parameters are tweaked such that the desired inductances are achieved for the inductors.

The *n2port* from the *analogLib* library is used as a model block for all the *ASITIC* inductors. Touchstone format of S-parameter file is used as file input of the *n2port* component since the actual S-parameters using *ASITIC* are given in touchstone format. The figures of merit such as conversion gain and noise figure are determined using *SpectreRF* in the *Analog Design Environment*.

A mixer's frequency converting action is characterized by conversion gain or loss. Voltage conversion gain is the ratio of the RMS voltages of the IF and RF signals, earlier given in Eq. (1) and (2). The variations of conversion gain with the power of LO signal ( $P_{LO}$ ) can be measured using *swept PSS (Periodic Steady-State) analysis* with *PAC (Periodic AC) analysis*. The *PAC analysis* will then compute the voltage conversion gain in dB20 of the whole circuit with *PORT3* as the output port (with output harmonic of 0, which is 5GHz) and *PORT1* as the input port (with input harmonic of -1, which is 0GHz). Setting the input port to *RF+* port, which is located after the balun circuit, will compute the voltage conversion gain of the mixer only. Simulation plots of the conversion gain swept from  $P_{LO} = -10\text{dBm}$  to  $P_{LO} = 30\text{dBm}$  are shown in **Figure 5-7**.

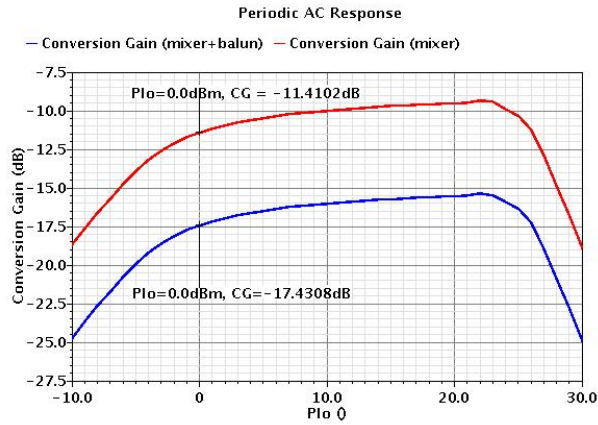


Figure 5; Conversion gain (in dB) vs.  $P_{LO}$  (w/o matching).

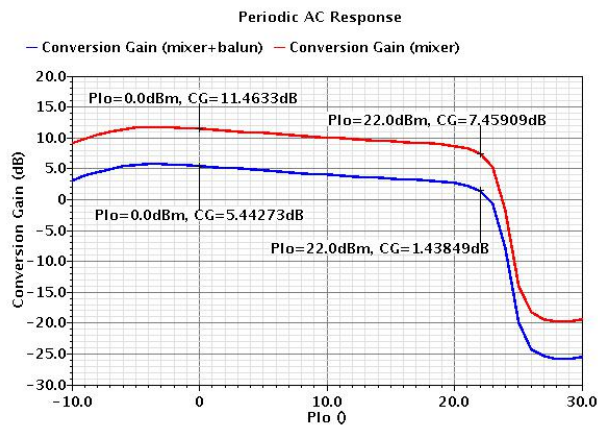


Figure 6; Conversion gain (in dB) vs.  $P_{LO}$  (ideal L).

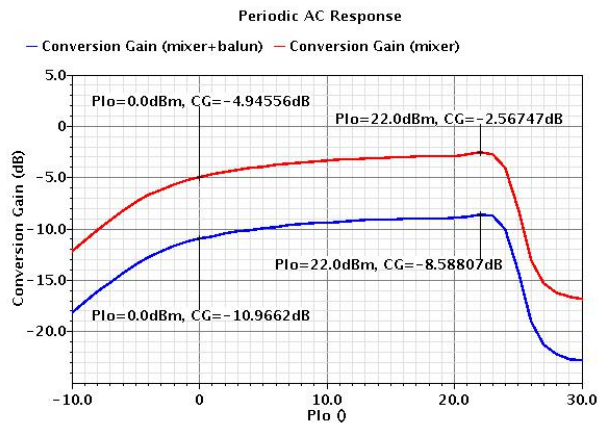
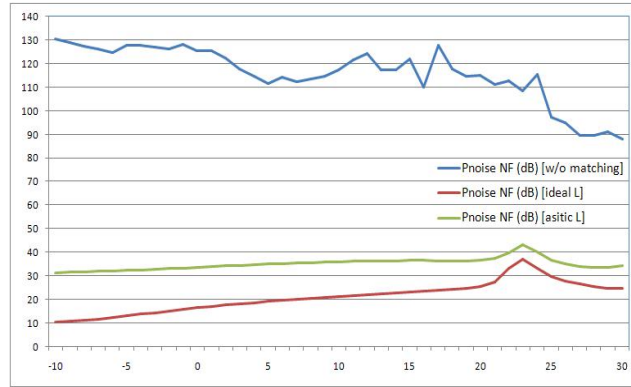
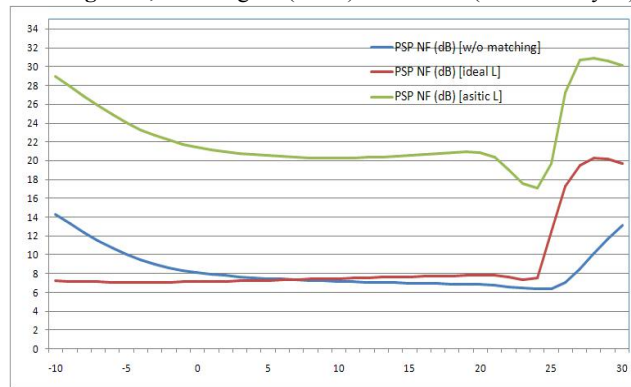


Figure 7; Conversion gain (in dB) vs.  $P_{LO}$  (ASITIC L).

For the noise figure,  $P_{noise}$  (Periodic Noise) analysis with PSS analysis is used. In addition,  $PSP$  (Periodic S-Parameters) analysis with PSS analysis can also be used to determine the noise figure of the circuit. Noise figure from a sweep range of -10dBm to 30dBm can now be determined and plotted using these analyses. The resulting plots are shown in Figure 8-9.



**Figure 8;** Noise figure (in dB) vs. PLO of (*Pnoise* analysis).



**Figure 9;** Noise figure (in dB) vs. PLO of (*PSP* analysis).

Table 5 summarizes the simulation results for conversion gain and noise figure at  $P_{LO} = 0\text{dBm}$ .

Figures of Merit	Value
<i>CG</i> (mixer+balun) [w/o matching]	-17.431dB
<i>CG</i> (mixer) [w/o matching]	-11.410dB
<i>CG</i> (mixer+balun) [ideal L]	5.443dB
<i>CG</i> (mixer) [ideal L]	11.463dB
<i>CG</i> (mixer+balun) [ <i>ASITIC</i> L]	-10.966dB
<i>CG</i> (mixer) [ <i>ASITIC</i> L]	-4.946dB
<i>Pnoise NF</i> [w/o matching]	125.355dB
<i>Pnoise NF</i> [ideal L]	16.529dB
<i>Pnoise NF</i> [ <i>ASITIC</i> L]	33.713dB
<i>PSP NF</i> [w/o matching]	8.127dB
<i>PSP NF</i> [ideal L]	7.136dB
<i>PSP NF</i> [ <i>ASITIC</i> L]	21.437dB

**Table 5.** Simulation results (at  $P_{LO} = 0$ ).

## 4. Discussion of Results

Based on the conversion gain simulation results as shown in **Figure 5-7** and in **Table 5**, input and output impedance matching contribute to better performance. Furthermore, using ideal inductors for impedance matching produced better performance as compared to using non-ideal *ASITIC* inductors through the *n2port*. It can be observed from the simulation plots that the conversion gain of the mixer only is higher than the conversion gain of the whole circuit consisting of the mixer and the balun. This is because the balun in the circuit, which is a passive balun, has insertion loss and thus incapable of producing gain and degrading the overall gain of the cascaded network.

Input and output impedance matching still contribute to better noise figure performance of the circuit, as indicated in **Figure 8-9** and **Table 5**. It can also be observed that using ideal inductors for impedance matching produced lower noise figure as compared to using non-ideal *ASITIC* inductors through the n2port model. The model block n2port introduces noise to the system, thus, adding to the total noise figure of the circuit

## 5. Conclusions and Recommendations

A design of direct-conversion double-balanced mixer was implemented and optimized on this paper. Proper biasing and sizing of all the transistors were necessary to ensure the required mode of operation for all the transistors. Conversion gain and noise figure were determined to measure the performance of the mixer design. These performance parameters can be optimized by introducing impedance matching in the circuit. The effect of the passive balun in the mixer design was also noted, resulting to the decrease in the conversion gain of the overall circuit. Ultimately, the direct-conversion double-balance mixer design achieved conversion gain of 11.463dB and noise figure of 16.529dB (using *Pnoise analysis*) at 5GHz, comparable to other mixer designs from past researches.

For future studies, an active balun can be used instead of passive balun. Active baluns are capable of producing gain and if cascaded in a double-balanced mixer to supply the differential RF and LO inputs, the overall performance of the mixer can be improved. Although active baluns are unidirectional converters, they are also used for their large bandwidth, which is beyond what non-ideal passive baluns can provide<sup>[8]</sup>.

## Acknowledgment

The author would like to thank Prof. Maria Theresa De Leon, Ph.D. and Prof. John Richard E. Hizon, Ph.D. of Microelectronics and Microprocessors Laboratory at University of the Philippines for the technical support during the course of the study, and to the STMicroelectronics Calamba NPI Team and the Management Team.

## References

1. B. Razavi, "RF microelectronics," Upper Saddle River, NJ, USA: Prentice Hall Press, 1998.
2. W. Namgoong and T. Meng, "Direct-conversion RF receiver design," *IEEE Transactions on Communications*, vol. 49, no. 3, March 2001.
3. Y. Zhou, C.P. Yoong, L.S. Weng, Y.J. Khoi, M.C.Y. Wah, K.A C. Moy, and D.W.T. Fatt, "A 5 GHz dual-mode WiMAX/WLAN direct-conversion receiver," in *Proc. IEEE International Symposium on Circuits and Systems*, May 2006.
4. J.G. Atallah, S. Rodriguez, L.R. Zeng, and M. Ismail, "A direct conversion WiMAX RF receiver front-end in CMOS technology," in *Proc. International Symposium on Signals, Circuits and Systems*, vol. 1, July 2007.
5. J. Y. Lyu and Z.M. Lin, "A 2~11 GHz direct-conversion mixer for WiMAX applications," *TENCON 2007 – IEEE Region 10 Conference*, pp. 1-4, October 2007.
6. T. Lee, "The design of CMOS radio-frequency integrated circuits," Cambridge: Cambridge University Press, 1998.
7. M. Voltti, T. Koivisto, and E. Tiiliharju, "Comparison of active and passive mixers," *18th European Conference on Circuit Theory and Design*, pp. 890-893. August 2007.
8. F.R. Gomez, M.T. de Leon, and C.R. Roque, "Active balun circuits for WiMAX receiver front-end," *TENCON 2010 – IEEE Region 10 Conference*, pp. 1156-1161, November 2010.
9. T. Tikka, J. Ryyanen, M. Hotti, and K. Halonen, "Design of a high linearity mixer for direct-conversion base-station receiver," in *Proc. IEEE International Symposium on Circuits and Systems*, May 2006.
10. K.W. Hamed, A.P. Freundorfer, and Y.M.M. Antar, "A monolithic double-balanced direct conversion mixer with an integrated wideband passive balun," *IEEE Journal of Solid-State Circuits*, vol. 40, no. 3, pp. 622-629, March 2005.
11. J. Park, C.H. Lee, B.S. Kim, and J. Laskar, "Design and analysis of low flicker-noise CMOS mixers for direct-conversion receivers," *IEEE Transactions on Microwave Theory and Techniques*, vol. 54, no. 12, December 2006.
12. F.R. Gomez, "Design of impedance matching networks for RF applications," *Asian Journal of Engineering and Technology*, vol. 6, no. 4, September 2018.
13. A.M. Niknejad and R.G. Meyer, "Analysis and optimization of monolithic inductors and transformers for RF ICs," in *Proc. IEEE Custom Integrated Circuits Conference*, Santa Clara, CA, pp. 375-378, May 1997.
14. R.G. Meyer and A.M. Niknejad, "ASITIC for Windows NT/2000," *Research in RFIC Design*,



[http://rfic.eecs.berkeley.edu/~niknejad/Asitic/grackle/cygwin\\_info.html](http://rfic.eecs.berkeley.edu/~niknejad/Asitic/grackle/cygwin_info.html).

15. Stanford Microwave Integrated Circuits Laboratory. Integrated Spiral Inductor Calculator, <http://www-smirc.stanford.edu/spiralCalc.html>.
16. M. del Mar Hershenson, S.S. Mohan, S.P. Boyd and T.H. Lee, "Optimization of inductor circuits via geometric programming," in Proc. Design Automation Conference, New Orleans, LA, pp. 994-998, June 1999.